Journal of Inflammation Research

Dovepress
open access to scientific and medical research

Open Access Full Text Article

ORIGINAL RESEARCH

Construction of circRNA-Mediated Immune-Related ceRNA Network and Identification of Circulating circRNAs as Diagnostic Biomarkers in Acute Ischemic Stroke

Xing-Zhi Wang[1,2], Shuo Li[3], Yun Liu[3], Gui-Yun Cui[2], Fu-Ling Yan[3]

[1]School of Medicine, Southeast University, Nanjing, Jiangsu, 210009, People's Republic of China; [2]Department of Neurology, The Affiliated Hospital of Xuzhou Medical University, Xuzhou, Jiangsu, 221006, People's Republic of China; [3]Department of Neurology, Affiliated ZhongDa Hospital, School of Medicine, Southeast University, Nanjing, Jiangsu, 210009, People's Republic of China

Correspondence: Fu-Ling Yan, Tel +861 391 396 9651, Fax +8602583262251, Email yanfuling218@163.com

Background and Purpose: Accumulating evidence suggests that circular RNAs (circRNAs) are involved in immune and inflammatory processes after acute ischemic stroke (AIS). However, the roles of circRNA-mediated competing endogenous RNA (ceRNA) in modulating immune inflammation of AIS have not yet been determined. This study aimed to construct a circRNA-mediated immune-related ceRNA network and identify novel circRNAs in AIS.

Methods: Microarray data were downloaded from the GEO database and further analysed by R software. Then, we constructed a circRNA-mediated ceRNA network based on interaction information from the bioinformatics database. A topological property analysis of the ceRNA network was conducted to screen novel circRNAs. Finally, we further applied quantitative real-time polymerase chain reaction (qRT-PCR) to two independent sets.

Results: We constructed an AIS immune-related ceRNA (AISIRC) network containing immune-related genes (IRGs), miRNAs, and circRNAs. Additionally, we extracted the subnetwork from the AISIRC network and screened six immune-related circRNAs. After identification and validation, we finally confirmed that plasma levels of circPTP4A2 and circTLK2 were significantly increased in AIS patients compared with both healthy control subjects (HCs) and transient ischemic attack (TIA) patients. Logistic regression and receiver-operating characteristic (ROC) curve analyses demonstrated that these two circRNAs may function as predictive and discriminative biomarkers for AIS. We also confirmed that plasma levels of circPTP4A2 were elevated in TIA patients compared with HCs and might be an independent risk factor for predicting TIA. Longitudinal analysis of circRNA expression up to 90 days after AIS indicated that the ability of circPTP4A2 and circTLK2 to monitor AIS dynamics was highly desirable.

Conclusion: In summary, the circRNA-mediated immune-related ceRNA network was successfully constructed, and two circulating circRNAs (circPTP4A2 and circTLK2) improved sensitivity for the diagnosis of AIS and could be considered diagnostic biomarkers.

Keywords: circular RNA, acute ischemic stroke, immune mechanism, competing endogenous RNA, biomarker

Introduction

Acute ischemic stroke (AIS) is characterized by high incidence, high mortality and high disability, and represents a serious public health problem in China.[1,2] Currently, the diagnosis of AIS mainly relies on clinical symptoms and neuroimaging examinations, including computed tomography (CT) and magnetic resonance imaging (MRI). However, CT has poor sensitivity for detecting early changes after AIS.[3] In addition, MRI requires a long imaging time, which could lead to missed opportunities for intravenous thrombolysis or mechanical thrombectomy. Thus, a rapid, accurate blood biomarker for diagnosing AIS is necessary. TIA is a transient episode of neurological dysfunction that produces stroke-like symptoms and is associated with an increased risk of early stroke.[4] The early identification of TIA can significantly mitigate the risk of stroke. However, current methods lack the ability to predict TIA patients. Accumulating evidence reveals that immunity and

Received: 31 March 2022
Accepted: 10 July 2022
Published: 17 July 2022

inflammation fulfill important roles in stroke-induced brain damage. Following ischemic stroke, neuronal necrosis and apoptosis occur due to significant blood flow reduction and disruption of glucose and oxygen supply, which can promote the inflammatory response caused by the release of reactive oxygen species (ROS), cytokines and chemokines. Neuroinflammation further promotes the release of multiple cytokines in peripheral blood.[5,6] Although several studies have attempted to identify inflammatory biomarkers (eg, high sensitivity C-reactive protein,[7] interleukin-6,[8] procalcitonin,[9] and matrix metalloproteinase-8)[10] for the diagnosis of ischaemic cerebrovascular disease, there are still no validated diagnostic biomarkers in clinical use. Therefore, identifying novel immune-inflammatory markers for the accurate prediction of AIS and TIA is strongly desired.

Circular RNAs (circRNAs) are a new class of endogenous non-coding RNAs with a continuous closed-loop structure that are produced by back-splicing and fusion of an upstream 3' splice site and a downstream 5' splice site.[11] Due to the lack of 5' caps and 3' poly-A tails, circRNAs are more resistant to RNase R treatment, have much longer half-lives, and present higher stability than linear RNAs.[12] Thus, circRNAs are ideal molecular biomarkers for diagnosis. Competing endogenous RNA (ceRNA) is the most common regulatory mechanism of circRNAs. Briefly, circRNAs can act as microRNAs (miRNAs) "sponges" and competitively bind to miRNAs by miRNA response elements, reducing target gene suppression mediated by miRNAs and regulating the expression of target genes.[13] Increasing evidence shows that circRNAs acting as ceRNAs may exert immunomodulatory properties in certain diseases. For instance, circRNA_09505 aggravates inflammation by acting as a ceRNA for miR-6089 via the AKT1/NF-κB signaling pathway in collagen-induced arthritis (CIA) mice.[14] CircGLIS2 acts as a "miRNA sponge" to suppress miR-671 expression, and subsequently activates NF-κB signaling and promotes the motility of colorectal cancer cells.[15] Indeed, our previous study identified three differentially expressed circRNAs (circFUNDC1, circPDS5B, and circCDC14A) that can serve as biomarkers for diagnosing AIS.[16] Further study revealed that circCDC14A played a critical role in the regulation of inflammatory reactions during AIS.[17] However, the role of circRNAs serving as ceRNAs in the immune and inflammatory mechanisms of AIS remains less studied. In addition, there are no published studies on the expression of circRNAs in TIA patients.

To address this point, we constructed an AIS immune-related ceRNA (AISIRC) network using microarray datasets along with miRNA–gene and miRNA–circRNA interactions that were derived from the miRWalk and circbank databases, respectively. Through protein–protein interaction (PPI) network analysis, we identified the hub genes and extracted subnetworks from the AISIRC network. Then, we validated upregulated circRNA expression from the subnetwork via reverse transcription-quantitative polymerase chain reaction (RT–qPCR) in two independent samples. Finally, we investigated the potential utility of candidate circRNAs as biomarkers for AIS and TIA and characterized their temporal profiles after AIS.

Materials and Methods

Microarray Collection

We retrieved three published expression datasets from the GEO database using the keyword "acute ischemia stroke" and the organism was limited to "*Homo sapiens*". Inclusion criteria were defined as follows: (1) AIS patients within 72 h after stroke onset. (2) The expression profiles of plasma or whole blood samples of AIS patients and healthy controls (HCs) are presented in the dataset. (3) All original data for the microarray analyses are available through the GEO database. Therefore, the gene expression profile (GSE16561),[18] the miRNA expression profile (GSE110993)[19] and the circRNA expression profile (GSE133768)[16] were downloaded for further research. The detailed information of these three datasets is described in Table 1, including GEO series accession number, platform type, sample size, and other information.

Table 1 Characteristics of the Expression Profiles in This Study

Dataset	Platform	Type	Sample Size		Author	Publication	Year
			Stroke	Control			
GSE16561	GPL6883	Gene	39	24	Barr et al[18]	*Neurology*	2010
GSE110993	GPL15456	miRNA	20	20	Tiedt et al[19]	*Circ Res*	2017
GSE133768	GPL21825	circRNA	3	3	Zuo et al[16]	*Stroke*	2020

Immune-Related Genes (IRGs)

We downloaded IRG data from the ImmPort database,[20] which has been annotated to the adaptive or innate immune response, and the InnateDB database,[21] which has been applied to facilitate studies of the human innate immune process. The list of 1793 IRGs was obtained from ImmPort, and 1375 IRGs were acquired from the InnateDB online database. Finally, the two datasets were merged and 2719 IRGs were obtained from the merged dataset. A detailed description of the IRGs is listed in Supplementary Material Table S1.

Differential Expression Analysis

For each dataset, raw expression data were read into R (version 4.1.0), quantile normalized, $\log_2$-transformed and probe annotations. The probe IDs of circRNA and miRNA were matched for interpretation using the circBase[22] and miRbase[23] databases, respectively. Thereafter, we utilized the "limma" R package (version 3.48.3)[24] to screen the differentially expressed circRNAs (DECs), differentially expressed miRNAs (DEMs), and differentially expressed genes (DEGs) in peripheral blood samples between AIS patients and healthy controls. As non-coding RNA and gene expression profiling have different variance characteristics, which could subsequently influence our statistical analyses in these three different datasets, we selected different statistical criteria for each dataset. Specifically, we defined a $P < 0.05$ and $|\log_2$ fold change (FC)$| > 0.5$ as statistical thresholds for screening DEGs and DEMs, and a $P < 0.05$ and $|\log_2$ fold change (FC)$| > 1.0$ as criteria for identifying DECs. Differentially expressed immune-related genes (DEIRGs) resulted from intersections between DEGs and IRGs. To visualize the differentially expressed analysis for each dataset, we constructed volcano plots and heatmap using the "ggplot2" R package (version 3.3.5; https://ggplot2.tidyverse.org/) and the "pheatmap" R package (version 1.0.12; https://cran.r-project.org/web/packages/pheatmap), respectively.

Functional and Pathway Enrichment Analysis

To determine the potential biological function and mechanism of DEIRGs, Gene Ontology (GO) and Kyoto Encyclopedia of Genes and Genomes (KEGG) pathway annotation were performed using the clusterProfiler R-package (version 4.2.0).[25] Categorical annotation was obtained from GO biological process (BP), cellular component (CC) and molecular function (MF), and pathway membership was supplied as KEGG pathways. GO or KEGG with an adjusted p-value <0.05 was defined as significant.

Construction of the ceRNA Network

To construct a comprehensive circRNA-associated competing endogenous RNA (ceRNA) network, we identified miRNAs targeting circRNAs and miRNAs targeting genes based on a bioinformatics database. Specifically, the miRWalk 3.0 database[26] was used to predict genes interacting with DEMs, which were then intersected with the DEIRGs to determine the DEM–DEIRG interaction pairs. The upstream circRNAs of DEMs were predicted using the circbank database[27] with conservative settings. Then, overlaps among these targeting circRNAs of DEMs and the DECs from GSE133768 were obtained for DEM–DEC interaction pairs. According to the ceRNA hypothesis, circRNA could act as a miRNA sponge to inhibit the functions of the miRNAs it binds to and subsequently facilitate downstream target gene expression.[28] Thus, the negatively correlated DEM–DEIRG interaction pairs and DEM–DEC interaction pairs were screened to construct a DEC–DEM–DEIRG interaction pairs. For the aforementioned interaction pairs, DEIRGs and DECs shared common DEMs, constituting the competing triplet pairs. Finally, a dysregulated AIS immune-related ceRNA (AISIRC) network was established using the DEC–DEM–DEIRG competing triplet pairs and visualized utilizing Cytoscape (version 3.8.2).[29]

PPI Network Analysis

The PPI network was constructed using the STRING database (version 11.5)[30] with a medium confidence threshold 0.4, and all active interaction sources. Visualization of the interaction network was performed using Cytoscape (version 3.8.2). Additionally, the topological features, including degree, betweenness, and closeness were analysed by CentiScaPe (version 2.2).[31]

Study Design and Participants

The present study is a single-centre, case–control, hospital-based study designed to assess the diagnostic values of circulating circRNAs in patients after AIS. From October 2021 to March 2022, all subjects were enrolled from the Affiliated Hospital of Xuzhou Medical University, which is a National Advanced Stroke Center affiliated with the China Stroke Association.

The inclusion criteria of this study were as follows: aged 18 years or older; first episode of AIS within 72 hours of symptom onset, or TIA; and written informed consent was obtained from all subjects or their legally authorized representatives. AIS was diagnosed as acute focal neurologic deficits persisting for more than 24 hours and confirmed by CT or MRI. TIA was defined as focal neurological deficits lasting less than 24 hours and absence of infarction on neuroimaging. The exclusion criteria of this study included a history of haemorrhagic infarction, chronic kidney/liver diseases, severe heart failure, acute myocardial infarction, peripheral arterial occlusive disease, active malignant disease, and inflammatory or infectious diseases. In addition, HCs were enrolled from physical examination centre volunteers at the same hospitals who had no history of stroke. After admission, complete baseline data on demographic characteristics, clinical features, medical history and diagnostic work-up were collected. In addition, all eligible patients received acute treatment, such as endovascular and intravenous thrombolytic therapies, anticoagulants and antiplatelet therapy, according to Chinese guidelines.

This study comprised two samples. The validation sample included 36 AIS patients and 36 HCs. The replication sample consisted of 200 AIS patients, 66 TIA patients and 100 HCs. HCs from the validation sample were matched to AIS patients for age, sex, smoking history, alcohol drinking, atrial fibrillation, hypertension, diabetes, and dyslipidemia.

Standard Protocol Approvals, Registrations, and Patient Consents

This experimental protocol was reviewed and approved by the Ethics Committee of the Affiliated Hospital of Xuzhou Medical University (approval ID: XYFY2021-KL107-01) and conducted in compliance with the ethical principles expressed in the Declaration of Helsinki, and this study was registered at the US National Institutes of Health (NIH) Clinical Trials Registry (Identifier: NCT 05098340). Written informed consent was obtained from all subjects or their legally authorized representatives.

Blood Sample Collection and RNA Isolation

All blood samples were immediately collected upon admission to the hospital and before any therapy was administered. Whole blood was drawn into EDTA-K_2 plasma tubes and centrifuged at 2000 × g for 10 minutes at 4 °C. Then, the plasma was saved and stored at −80 °C in individual RNAase-free Eppendorf tubes until RNA extraction. Total RNA was isolated from plasma with TRIzol LS reagent (Invitrogen, Carlsbad, CA, USA) according to the manufacturer's protocol. Synthetic *Caenorhabditis elegans* miR-39-3p (cel-miR-39-3p, RiBoBio, Guangzhou, China) was used as an exogenous reference gene to normalize sample-to-sample variation. To increase the yield of RNA isolation from plasma, glycogen (Invitrogen) at a final concentration of 100 μg/mL was added per sample during RNA precipitation. The purity and concentration of the total RNA were determined using a NanoPhotometer® spectrophotometer (IMPLEN, CA, USA).

qRT-PCR

The total RNA of plasma was reverse transcribed into complementary DNA (cDNA) using the HiScript® Q RT SuperMix for qPCR Kit (R123-01, Vazyme, Nanjing, China) following the manufacturer's manuals. Subsequently, qPCR was performed using the UltraSYBR Mixture (CWBIO, Beijing, China) on the BioRad CFX96™ Real-Time System. For circRNA analysis, each qRT-PCR was performed in a total volume of 50 μL including 25 μL 2 × UltraSYBR mixture, 1 μL forward primer (10 μM), 1 μL reverse primer (10 μM), and 2 μL cDNA template. The qRT-PCR cycling conditions were as follows: 95 °C for 10 minutes, 40 cycles of 95 °C for 15 seconds, and 60 °C for 1 minute. Glyceraldehyde-3-phosphate dehydrogenase (GAPDH) was used for internal normalization. All samples were analysed in triplicate. The relative expression of circRNAs was calculated using the $2^{-\Delta\Delta Ct}$ method. The primers for qRT-PCR are described in Supplementary Material Table S2 and were synthesized by RiBoBio (Guangzhou, China).

Statistical Analysis

All data were statistically analysed using SPSS 26.0 statistics software (IBM corporation, CA, USA). The normality of distributions was assessed by using the Kolmogorov–Smirnov test. Continuous variables with normal distribution are described as the mean ± standard deviation (SD), whereas variables with a skewed distribution are represented as the median (interquartile range; IQR). For two-group comparisons of continuous variables, we performed Student's *t*-test (normally distributed data) or Mann–Whitney *U*-test (nonnormally distributed data). For multiple comparisons of continuous variables, one-way ANOVA (normally distributed data) or Kruskal–Wallis ANOVA (nonnormally distributed data) was used. Categorical variables are presented as percentages and proportions and were analysed using Pearson's chi-squared test or Fisher's exact test. For statistics from qRT-PCR, fold change (FC) values of circRNAs were measured to represent relative expression levels. To assess the role of candidate circRNAs as independent predictors of AIS, logistic regression models were used to identify circRNAs associated with stroke in the replication sample. For multivariate logistic regression, each model tested the relationship between the circRNAs and AIS diagnosis while adjusting for confounding factors, such as sex, age, hypertension, diabetes mellitus and biochemical indexes. The diagnostic property of each validated circRNA for AIS was evaluated by receiver operating characteristic (ROC) analysis, and the diagnostic accuracy was subsequently assessed by calculating the area under the curve (AUC). The optimal cut-off values of candidate circRNAs were determined according to the Youden criteria. To assess the joint predictive ability of candidate circRNAs, we applied binary logistic regression to calculate the predicted values of each subject, and subsequently used these results as the probability to construct ROC curves. For all analyses, statistical significance was defined as $P < 0.05$. If appropriate, a conservative Bonferroni correction multiple hypothesis test was applied.

Results

Identification of DEIRGs, DEMs, and DECs in AIS

To identify immune-related biomarkers and validate potential candidate circRNAs in AIS, we analysed three expression datasets from the GEO database. The flow diagram of the study is shown in Figure 1. Based on the cut-off criteria ($P < 0.05$ and $|\log_2$ fold change (FC)$| > 0.5$), we screened 169 DEGs from the GSE16561 dataset, and 63 DEMs from the GSE110993 dataset (Figure 2A–D). Of the169 DEGs, 97 were upregulated and 72 were downregulated. Among the 63 DEMs, a total of 32 human mature miRNAs (16 upregulated and 16 downregulated), and 31 pre-miRNAs (18 upregulated and 13 downregulated) were identified. Subsequently, 32 mature DEMs were selected for further investigation. Next, we set a $P < 0.05$ and $|\log_2$ fold change (FC)$| > 1.0$ as statistical criteria for identifying DECs. Then, a total of 548 DECs were identified from the GSE133768 dataset, including 225 upregulated circRNAs and 323 downregulated circRNAs (Figure 2E and F). A detailed description of the differential expression analysis is listed in Supplementary Material Tables S3–S5. Immune responses play important roles in the pathophysiology of ischemic stroke.[5] We thus focused on 2719 IRGs obtained from the ImmPort[20] and InnateDB[21] online databases. Finally, 52 DEIRGs were generated by a cross between DEGs and IRGs (Figure 2G, Supplementary Material Table S6).

Functional Analysis of the DEIRGs

Although 52 DEIRGs were identified based on two immunologically relevant gene databases and a gene expression profile of ischemic stroke from the GEO database, their underlying biological function and mechanism remain unknown. Thus, further investigations of their cellular functions are warranted to construct an AIS immune-related ceRNA (AISIRC) network. Specifically, GO and KEGG pathway enrichment analyses were used to annotate the functions of these 52 DEIRGs. Eventually, a total of 172 GO terms and 8 KEGG pathways were found to be significantly enriched for DEIRGs (Supplementary Material Tables S7–S8). These DEIRGs were mostly enriched in critical immune-related biological processes such as immune response-activating cell surface receptor signaling pathway, immune response-activating signal transduction, neutrophil activation involved in immune response, and neutrophil-mediated immunity. The DEIRGs were mainly involved in several immune-related molecular functions, including immune receptor activity, cytokine receptor activity, and IgG binding, while they participated in some specific cellular components, such as specific granule and tertiary granule (Figure 3A). Additionally, several significantly enriched KEGG pathways for DEIRGs were

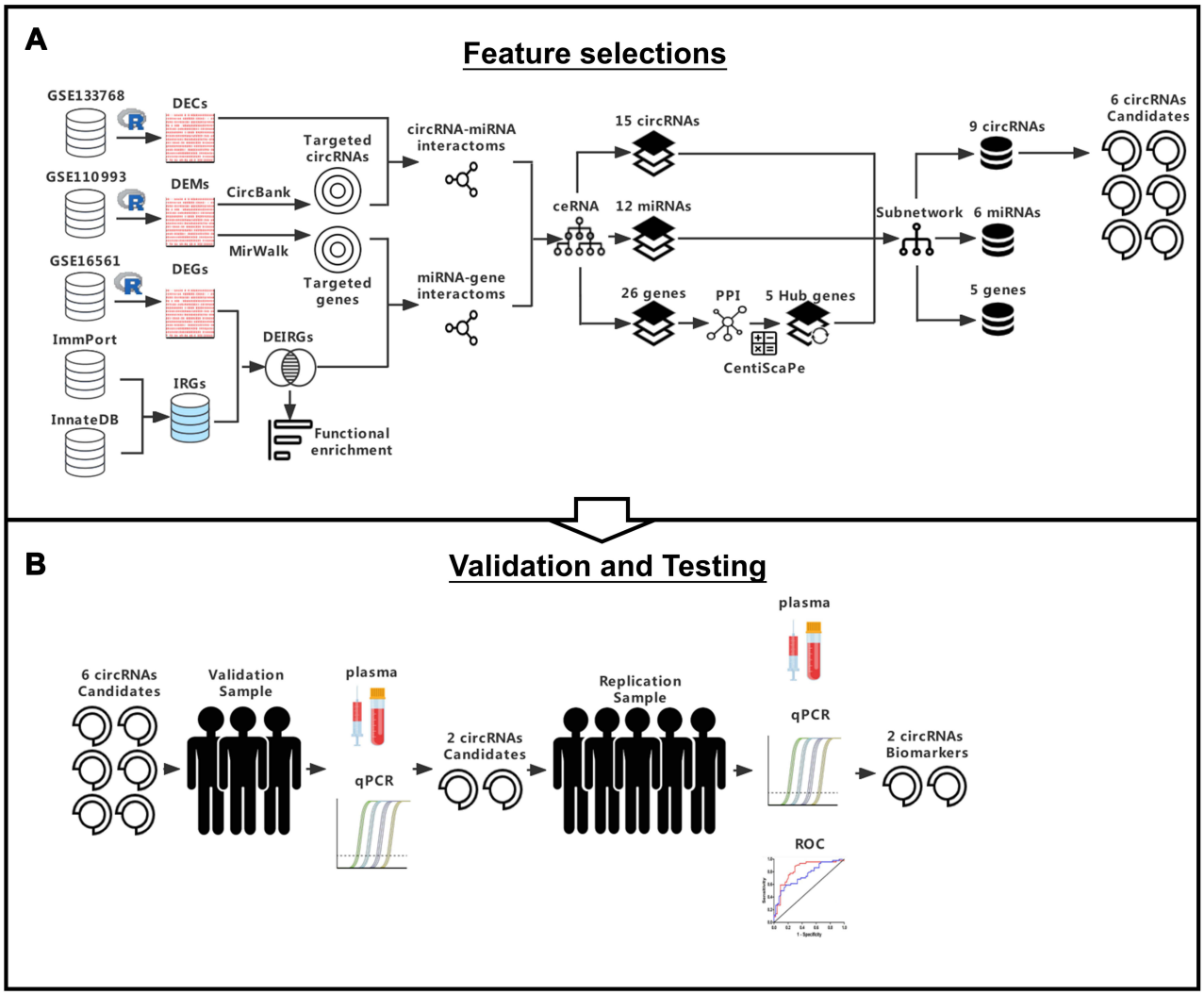

Figure 1 Flow diagram for the identification of immune-related circRNA biomarkers in AIS. (**A**) DECs, DEMs, DEIRGS were obtained from three different GEO datasets and two publicly accessible databases, and were analyzed by "limma" R package. The ceRNA pairs were predicted using Circbank and Mirwalk online databases, then constructed the ceRNA network. Identification the hub genes of the ceRNA network by centiscape algorithm and were further constructed the sub ceRNA network. The six highly expressed circRNAs were chosen as candidates for further investigation. (**B**) These six candidate circRNAs analyzed by qPCR and ROC curves in validation sample for functional validation. Finally, two circRNAs biomarkers were used to test the predictive accuracy in replication sample.

associated with the immune response, including cytokine–cytokine receptor interaction, primary immunodeficiency, Th17 cell differentiation, Th1 and Th2 cell differentiation and T cell receptor signaling pathway (Figure 3B). The results above indicated that these 52 DEIRGs might be involved in the immune response induced by ischemic stroke.

Construction of an AISIRC Network

To further illustrate the potential regulatory relationship between DEIRGs, DEMs and DECs, we constructed an AISIRC network according to the ceRNA hypothesis. The process of AISIRC network construction is detailed in Figure 1A. Based on the DEM–DEIRG interaction pairs and the DEM–DEC interaction pairs, DECs and DEIRGs regulated by the same DEMs were screened. In total, a significantly dysregulated AISIRC network was constructed containing 53 nodes (including 10 upregulated DECs, 5 downregulated DECs, 4 upregulated DEMs, 8 downregulated DEMs, 19 upregulated DEIRGs, and 7 downregulated DEIRGs) and 56 edges (Figure 4; Supplementary Material Tables S9–S10).

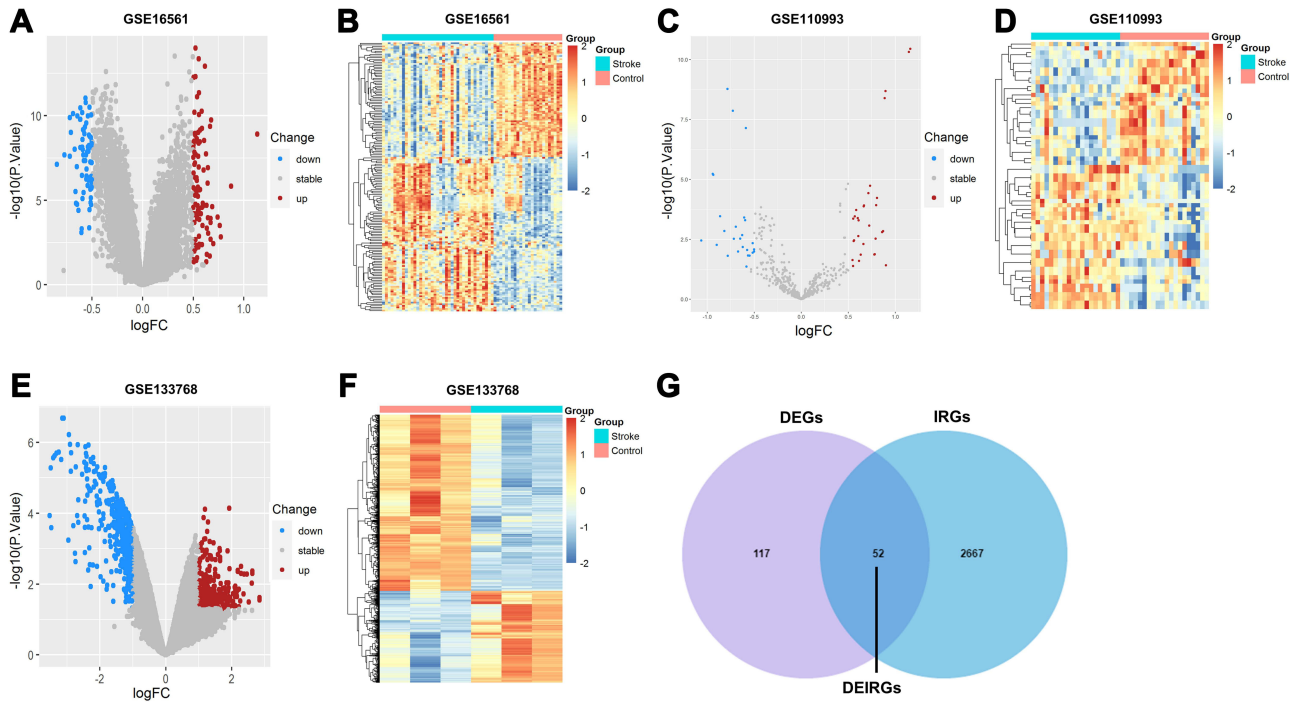

Figure 2 Screening and identification of DEGs, DEMs, DECs and DEIRGs in AIS patients and HCs. The volcano plot of DEGs (**A**), DEMs (**C**), DECs (**E**) in GSE16561, GSE110993, and GSE133768, respectively. Red dots represent upregulation while blue dots represent downregulation. The hierarchical cluster heatmaps of DEGs (**B**), DEMs (**D**), DECs (**F**) in GSE16561, GSE110993, and GSE133768, respectively. Orange red represents high expression while blue represents low expression. (**G**) Venn diagram of DEGs and IRGs. Purple and blue circles represent DEGs and IRGs, respectively, and their overlap region represents DEIRGs.

PPI Analyses and Subnetwork Construction

To further analyse the interactions of proteins encoded by these 26 DEIRGs in the AISIRC network, we constructed a PPI network using the STRING database and Cytoscape software. After removing unconnected nodes, the final PPI network contained 21 nodes and 39 edges (Figure 5A). When analysing the topological characteristics of all nodes, five DEIRGs showed degree, betweenness, and closeness above the average levels calculated on the whole PPI network, ultimately acting as potential hub genes (Figure 5A and Table 2).

To identify immune-related circRNAs, we selected the five aforementioned hub genes as seed nodes to extract two circRNA–miRNA–hub gene subnetworks from the AISIRC network (Figure 5B). In total, nine circRNA, six miRNA and five gene nodes were identified in the subnetworks. As these nodes were likely to be key parts of the AISIRC, we hypothesized that these nine circRNAs may be the potential biomarkers of poststroke immune responses. Eventually, we selected six upregulated circRNAs (hsa_circ_0000479, hsa_circ_0047460, hsa_circ_0007364, hsa_circ_0017252, hsa_circ_0008420, and hsa_circ_0045128) as candidate biomarkers for further study.

Differentially Expressed circRNAs in the Study Sample

The baseline characteristics of the validation and replication samples are depicted in Table 3. AIS patients and HCs were well matched in the validation samples apart from a higher serum glucose level in the AIS group. In the replication sample, the prevalence of hypertension, diabetes mellitus and atrial fibrillation, serum glucose and LDL levels exhibited a significant increase in AIS patients compared with HCs, and the prevalence of hypertension was also higher in TIA patients than HCs. In addition, the prevalence of atrial fibrillation and serum glucose levels demonstrated a significant increase in AIS patients compared with TIA patients, while the prevalence of dyslipidemia showed a slight reduction in the replication sample.

Among the six candidate circRNAs, a reliable PCR primer of hsa_circ_0008420 could not be designed due to its low GC content. The remaining five circRNAs were further analysed by qRT-PCR in the validation sample. Among

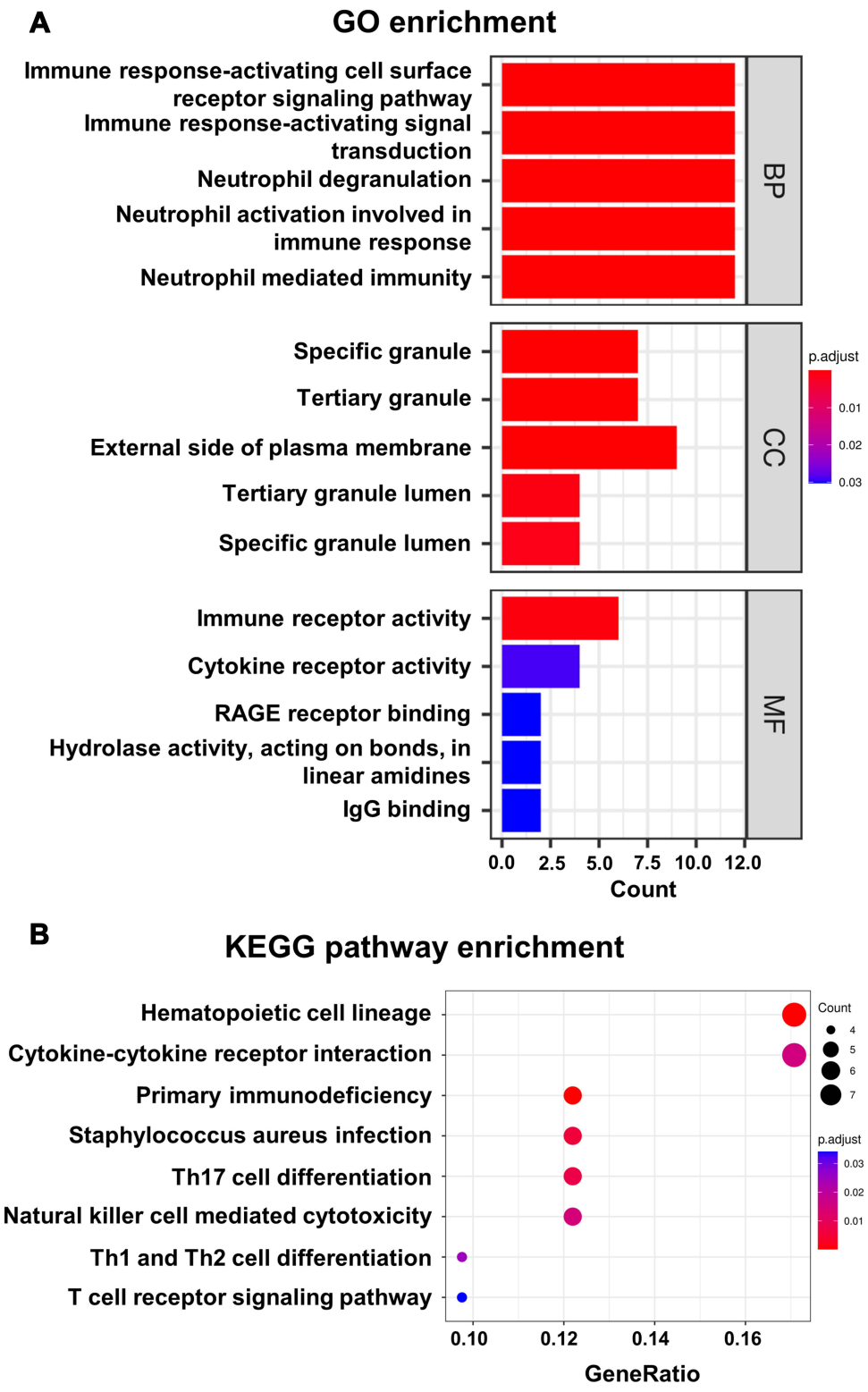

Figure 3 Functional enrichment analysis for DEIRGs. (**A**) Top 15 significantly enriched GO terms for biological process (BP), cellular component (CC), and molecular function (MF). The color scale from blue to red indicates the gradual increase of the level of enrichment. (**B**) KEGG pathway enrichment analyses of DEIRGs. The color scale from blue to red indicates the gradual increase of the level of enrichment. Each circle indicates a specific KEGG pathway terms and circle size represents the number of genes that have been enriched.

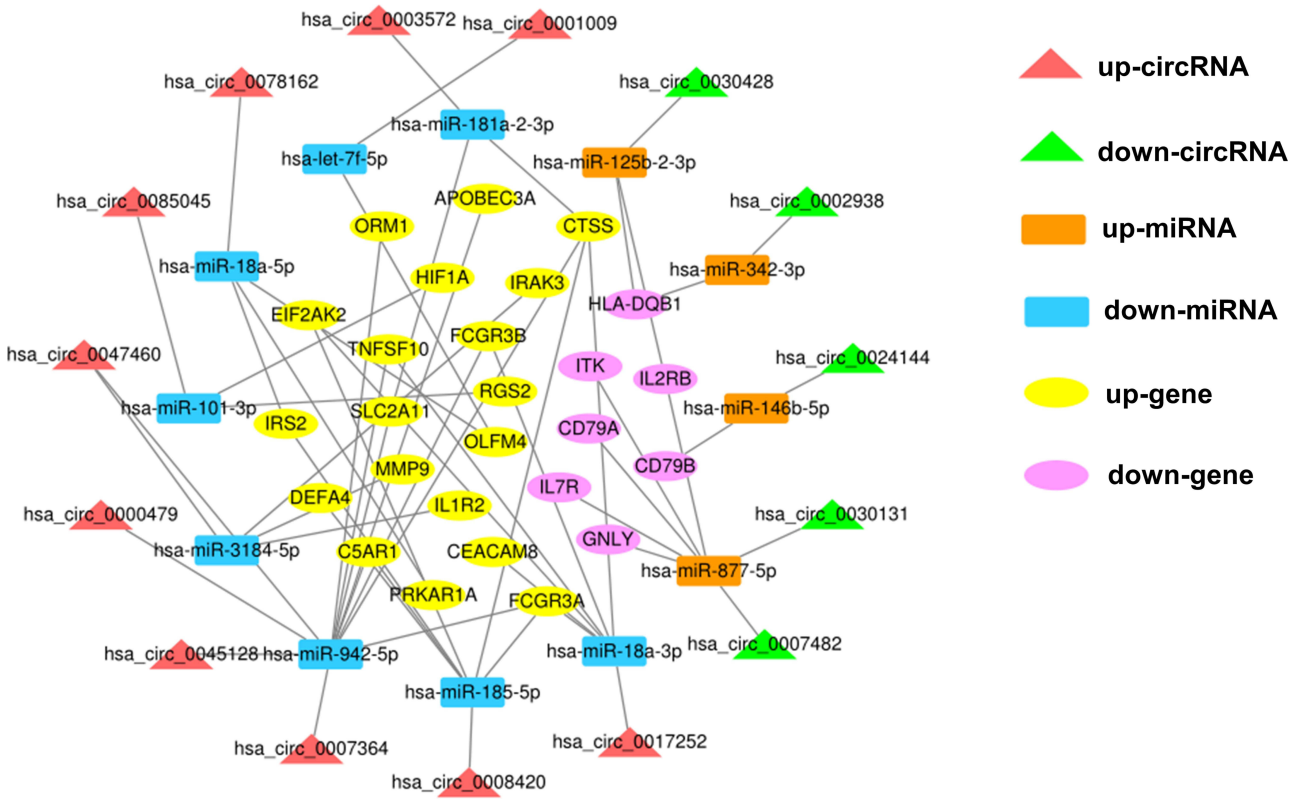

Figure 4 Construction of the dysregulated AISIRC network in AIS. Red and green triangles represent upregulated circRNAs and downregulated circRNAs, respectively. Orange and blue rectangles represent upregulated miRNAs and downregulated miRNAs, respectively. Yellow and purple ovals represent upregulated genes and downregulated genes, respectively. Gray lines represent the interactions between the parts of AISIRC network.

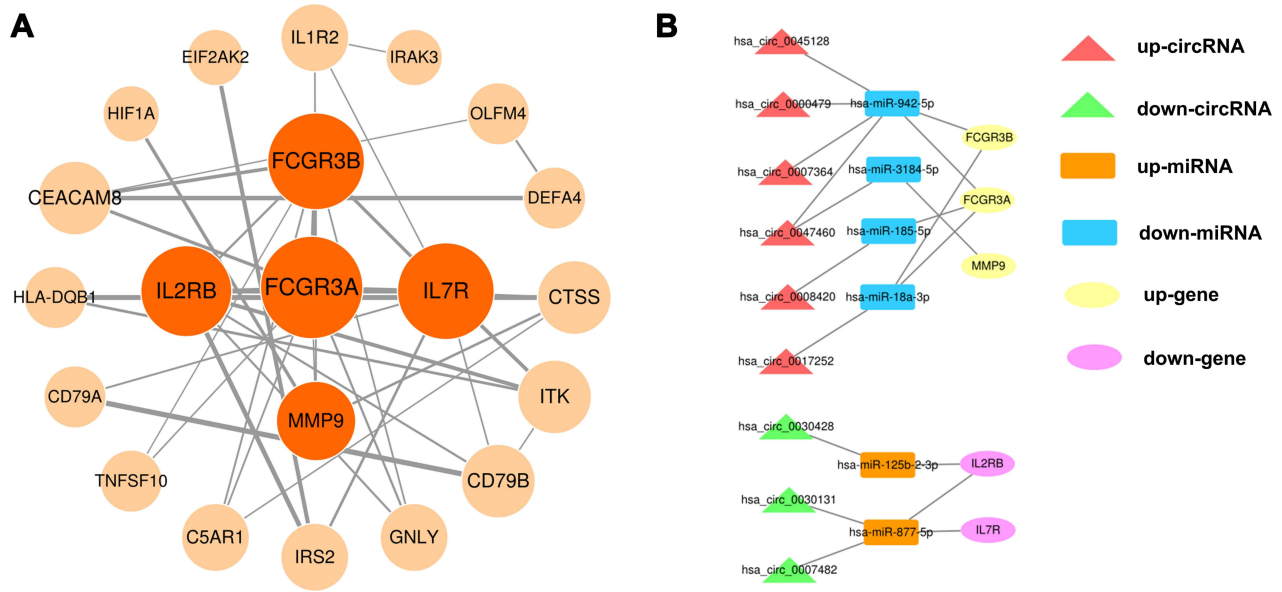

Figure 5 Construction of the PPI network and the circRNA–miRNA–hub gene subnetwork. (**A**) PPI network of DEIRGs in the AISIRC network. Node size is proportional to their degree in the PPI network, and edge thickness is proportional to the combined score between DEIRGs. The five important hub genes (dark orange nodes) were identified from the PPI network using the Centiscape algorithm. (**B**) Subnetworks of these five hub genes extracted from the AISIRC network. Red and green triangles represent upregulated circRNAs and downregulated circRNAs, respectively. Orange and blue rectangles represent upregulated miRNAs and downregulated miRNAs, respectively. Yellow and purple ovals represent upregulated genes and downregulated genes, respectively. Gray lines represent the interactions between the parts of AISIRC network.

Table 2 Five Hub Genes Identified by Centiscape 2.2

Gene Name	Degree	Betweenness	Closeness	Gene Descriptions
FCGR3A	9	112.70	0.030	Low-affinity immunoglobulin gamma Fc region receptor III-A
FCGR3B	8	81.30	0.029	Low-affinity immunoglobulin gamma Fc region receptor III-B
IL7R	8	116.57	0.029	Interleukin-7 receptor subunit alpha
IL2RB	7	54.47	0.027	High-affinity IL-2 receptor subunit beta
MMP9	5	61.07	0.023	Matrix metalloproteinase-9

them, hsa_circ_0007364 and hsa_circ_0045128 were differentially regulated ($P < 0.01$ after Bonferroni correction), and they were all upregulated in patients with AIS compared with HCs: hsa_circ_0007364 ($P = 0.0002$, Mann–Whitney *U*-test) and hsa_circ_0045128 ($P = 0.0026$, Mann–Whitney *U*-test) (Figure 6). The other circRNAs, including hsa_circ_0000479, hsa_circ_0047460 and hsa_circ_0017252, did not show significant differences in gene expression levels (Figure 6). According to the circBase database[22] and NCBI reference sequence, hsa_circ_0007364 is derived from the back-splicing of exon 2–3 of protein tyrosine phosphatase 4A2 (PTP4A2), and hsa_circ_0045128 is derived from the back-splicing of exon 7–11 of tousled like kinase 2 (TLK2). Therefore, we refer to hsa_circ_0007364 and hsa_circ_0045128 as circPTP4A2 (circular RNA PTP4A2) and circTLK2 (circular RNA TLK2), respectively. To further validate these results, we next examined the circulating levels of circPTP4A2 and circTLK2 in another independent sample (including 200 AIS patients, 66 TIA patients and 100 HCs) that was referred to as the replication sample. As the distribution of relative expression levels for circPTP4A2 and circTLK2 were skewed, these quantitative variables are presented as medians and interquartile ranges. Both circPTP4A2 and circTLK2 demonstrated significantly higher expression levels in AIS patients than in HCs: circPTP4A2 (median=1.85, IQR=1.29; $P=6.66\times10^{-15}$; Figure 7A) and circTLK2 (median=1.61, IQR=1.11; $P=1.41\times10^{-10}$; Figure 7B). In addition, their expression levels were also upregulated in AIS patients compared with TIA patients: circPTP4A2 (median=1.39, IQR=0.54; $P=0.004$; Figure 7A) and circTLK2 (median=1.11, IQR=1.74; $P=0.001$; Figure 7B). Moreover, the relative expression level of circPTP4A2 (median=1.39, IQR=0.54; $P=0.003$; Figure 7A) was increased in patients with TIA compared with HCs.

Diagnostic Performance of circPTP4A2 and circTLK2

To further evaluate the diagnostic potential of circPTP4A2 and circTLK2 for AIS and TIA, univariate and multivariate logistic regression analyses were performed in the replication sample (Table 4). First, we treated the AIS, TIA and HCs groups as a three-category variable and employed the HCs group as a reference category. In the univariate analyses, both circPTP4A2 and circTLK2 expression levels independently correlate with AIS and TIA presence. After adjusting for age, sex, vascular risk factors and biochemical indexes on admission, the multivariate analysis revealed that circPTP4A2 and circTLK2 expression levels remained associated with AIS and TIA. Subsequently, we employed the TIA group as a reference category. In the univariate analyses, the circPTP4A2 and circTLK2 levels were still independently correlated with AIS presence. After adjusting for age, sex, vascular risk factors and biochemical indexes on admission, the multivariable analysis revealed that circPTP4A2 and circTLK2 expression levels remained associated with AIS. The odds ratios (ORs) and 95% confidence intervals (CIs) of circRNAs for AIS or TIA are detailed in Table 4.

To further evaluate the diagnostic properties of circPTP4A2 and circTLK2 for AIS and TIA, ROC curve analyses were performed in the replication sample (Figure 8 and Table 5). The AUCs of circPTP4A2 and circTLK2 for differentiating between HCs and AIS were 0.762 (95% CI: 0.703–0.820, $P<0.001$) and 0.734 (95% CI: 0.675–0.793, $P<0.001$), respectively. The combination of these two circRNAs showed a markedly higher AUC value (AUC=0.805, 95% CI: 0.751–0.860, $P<0.001$) than the individual circRNAs for AIS identification, corresponding to a sensitivity of 90% and a specificity of 63%. Among 200 AIS patients from the replication sample, 157 patients had positive results from the initial CT scans. Therefore, the sensitivity of initial CT scan was 78.5% (157/200), which was lower than that

Table 3 Baseline Characteristics of the Validation and Replication Sample

Baseline Characteristics	Validation Sample			Replication Sample					
	AIS	HCs	*P*-value[a]	AIS	TIA	HCs	*P*-value[a]	*P*-value[b]	*P*-value[c]
Demographics									
Total, n	36	36	-	200	66	100	-	-	-
Age, mean (SD), years	61.8(12.6)	65.8(11.9)	0.177*	64.8(10.7)	65.0(11.0)	64.9(11.3)	0.999[§]	0.989[§]	0.991[§]
Female, n (%)	16(44.4)	15(41.7)	0.812[†]	67(33.5)	27(40.9)	43(43)	0.107[†]	0.789[†]	0.275[†]
Vascular risk factors, n(%)									
Hypertension	21(58.3)	16(44.4)	0.238[†]	134(67)	40(60.6)	43(43)	<0.001[†]	0.026[†]	0.344[†]
Diabetes mellitus	9(25)	6(16.7)	0.384[†]	58(29)	17(25.8)	15(15)	0.008[†]	0.086[†]	0.612[†]
Dyslipidemia	11(30.6)	8(22.2)	0.422[†]	47(23.5)	24(36.4)	24(24)	0.923[†]	0.086[†]	0.041[†]
Atrial fibrillation	4(11.1)	1(2.8)	0.164[†]	34(17)	1(1.5)	1(1)	<0.001[†]	0.766[†]	0.001[†]
Coronary artery disease	3(8.3)	4(11.1)	0.691[†]	32(16)	14(21.2)	11(11)	0.244[†]	0.072[†]	0.332[†]
Smoking history	9(25)	5(13.9)	0.234[†]	40(20)	14(21.2)	13(13)	0.134[†]	0.161[†]	0.832[†]
Alcohol	2(5.6)	1(2.8)	0.555[†]	13(6.5)	4(6.1)	3(3)	0.203[†]	0.337[†]	0.899[†]
Biochemical indexes on admission, mean (SD)/median (interquartile range)									
Serum glucose, mmol/L	5.82(2.49)	5.23(1.15)	0.024[‡]	5.96(2.13)	5.27(1.39)	5.36(1.17)	<0.001[§]	0.980[§]	<0.001[§]
Triglycerides, mmol/L	1.27(0.71)	1.27(0.78)	0.434[‡]	1.26(0.85)	1.29(0.93)	1.18(0.74)	0.210[§]	0.335[§]	0.559[§]
Total cholesterol, mmol/L	4.32(1.10)	4.40(0.93)	0.736*	4.33(1.04)	4.11(0.97)	4.13(0.98)	0.099[▽]	0.938[▽]	0.131[▽]
HDL, mmol/L	1.04(0.38)	1.29(0.64)	0.161[‡]	1.04(0.30)	1.04(0.37)	1.05(0.43)	0.210[§]	0.335[§]	0.559[§]
LDL, mmol/L	2.76(0.74)	2.58(0.79)	0.329*	2.66(1.17)	2.54(1.16)	2.38(1.07)	0.008[§]	0.502[§]	0.365[§]

Notes: [a]AIS patients vs HCs; [b]TIA patients vs HCs; [c]AIS patients vs TIA patients; *Student's *t*-test; [†]Chi-squared test; [‡]Mann–Whitney *U*-test; [§]Kruskal–Wallis ANOVA test; [▽]one-way ANOVA test.
Abbreviations: AIS, acute ischemic stroke; HCs, healthy control subjects; HDL, high-density lipoprotein; LDL, low-density lipoprotein; SD, standard deviation; TIA, transient ischemic attack.

https://doi.org/10.2147/JIR.S368417

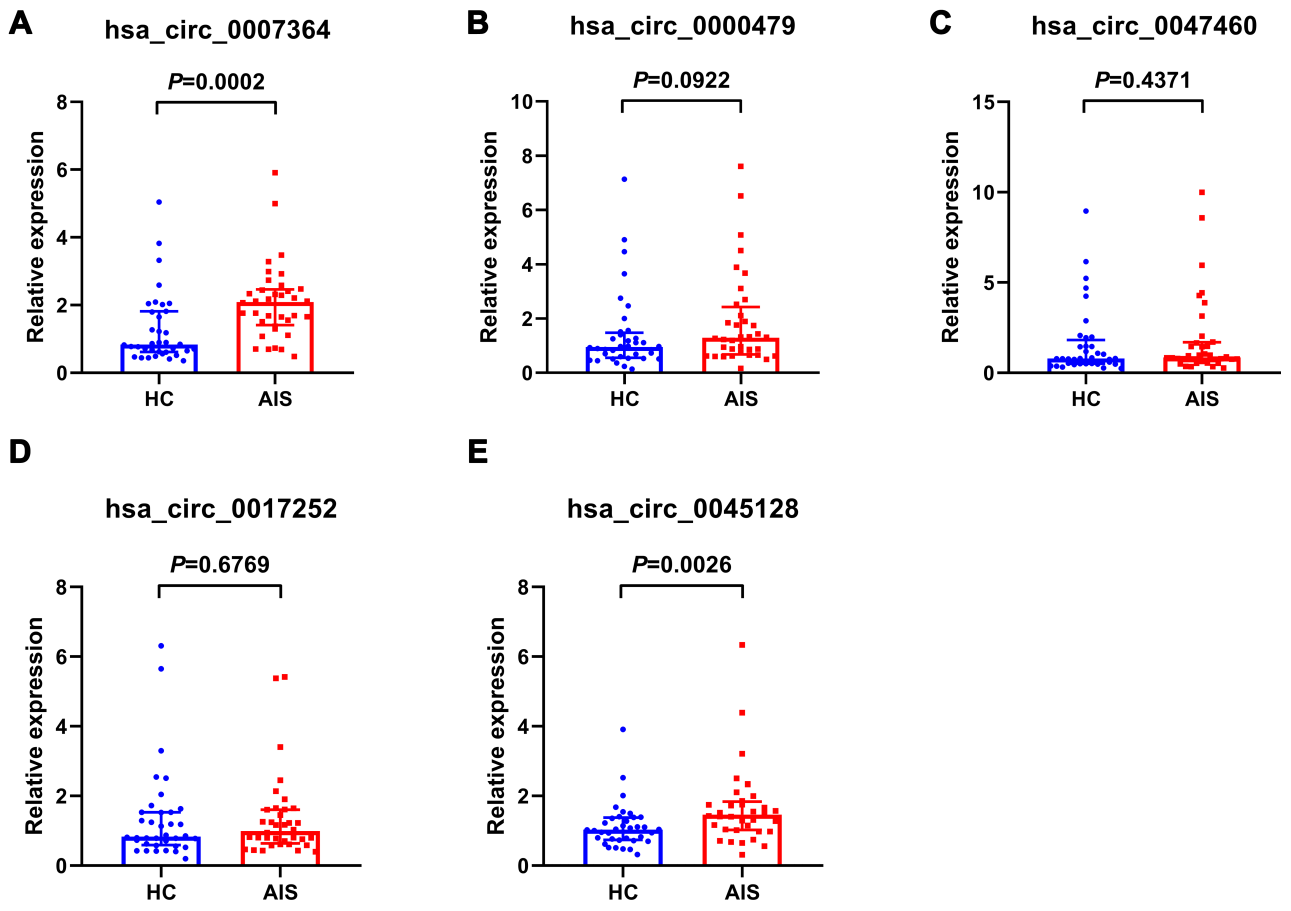

Figure 6 Relative levels of the five candidate circRNAs via qRT-PCR in the validation sample (n=36/36, healthy control [HC]/acute ischemic stroke [AIS]). Two circRNAs were significantly differentially expressed: (**A**) hsa_circ_0007364 and (**E**) hsa_circ_0045128. Three circRNAs were not significantly differentially expressed: (**B**) hsa_circ_0000479, (**C**) hsa_circ_0047460, and (**D**) hsa_circ_0017252. Median ± interquartile range, Mann–Whitney *U*-test.

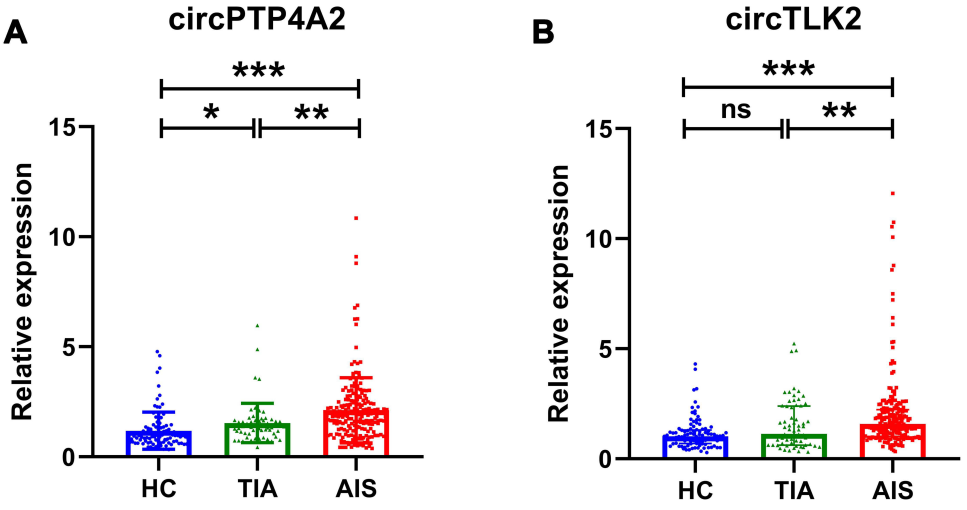

Figure 7 Relative levels of (**A**) circPTP4A2 and (**B**) circTLK2 via qRT-PCR in the replication sample (n=100/66/200, healthy control [HC]/transient ischemic attack [TIA]/acute ischemic stroke [AIS]). Median ± interquartile range, Kruskal–Wallis ANOVA test followed by Bonferroni correction pairwise comparisons. *$P < 0.05$; **$P < 0.01$; ***$P < 0.001$.

Abbreviation: ns, not significant.

Table 4 Logistic Regression Analysis for Predictive Power of circPTP4A2 and circTLK2

Variable	Univariate Analysis[a]		Multivariate Analysis[b]	
	OR (95% CI)	*P*-value	OR (95% CI)	*P*-value
AIS[c]				
circPTP4A2	3.204 (2.183–4.705)	<0.001	2.788(1.876–4.145)	<0.001
circTLK2	2.576 (1.768–3.754)	<0.001	2.480(1.676–3.670)	<0.001
TIA[c]				
circPTP4A2	1.782 (1.142–2.780)	0.011	1.628(1.036–2.560)	0.035
circTLK2	1.877 (1.230–2.863)	0.003	1.736(1.141–2.639)	0.010
AIS[d]				
circPTP4A2	1.799 (1.291–2.505)	0.001	1.713(1.220–2.405)	0.002
circTLK2	1.373 (1.045–1.804)	0.023	1.429(1.078–1.894)	0.013

Notes: [a]Only one of the candidate circRNAs was included in the model. [b]The age, sex, vascular risk factors and biochemical indexes were adjusted in the model. [c]The reference category was the HCs group. [d]The reference category was the TIA group.
Abbreviations: AIS, acute ischemic stroke; CI, confidence interval; HCs, healthy control subjects; OR, odds ratio; TIA, transient ischemic attack.

obtained with the set of combined circRNAs (sensitivity=90%). Furthermore, the AUCs of circPTP4A2 and circTLK2 for differentiating between HCs and TIA were 0.708 (95% CI: 0.628–0.787, $P<0.001$) and 0.564 (95% CI: 0.470–0.658, $P=0.164$), respectively. The AUC of the combination of circPTP4A2 and circTLK2 for TIA identification was 0.664 (95% CI: 0.580–0.748, $P<0.001$). Ultimately, we observed that the AUC was 0.704 for circPTP4A2 and 0.632 for circTLK2 in distinguishing AIS patients from TIA patients. The AUC of the combination of these two circRNAs (AUC=0.707, 95% CI: 0.640–0.773, $P<0.001$) was slightly but not significantly higher than that of circPTP4A2.

Temporal Profile of circPTP4A2 and circTLK2 Levels After AIS

To further test the clinical stability of circPTP4A2 and circTLK2 as biomarkers of AIS, we examined their expression levels on Days 1, 2, 3, 7 and 90 after stroke. We collected data at these five time points from 18 AIS patients as study samples. In addition, 18 plasma samples from HCs were used as controls. As shown in Figure 9, the relative expression of circPTP4A2 and circTLK2 varied with time in AIS patients compared with HCs. We observed circPTP4A2 and circTLK2 were higher in AIS samples collected at Day 1 than in HCs (circPTP4A2: $P=0.010$; circTLK2: $P<0.001$). Furthermore, the relative expression of circPTP4A2 gradually declined from Day 2 to Day 90 after AIS. In contrast, the relative expression of circTLK2 declined rapidly from Day 1 to Day 2 after AIS ($P<0.001$), and subsequently gradually increased until Day 7 after stroke. Furthermore, the expression level of circTLK2 in AIS samples at Day 2 and Day 3

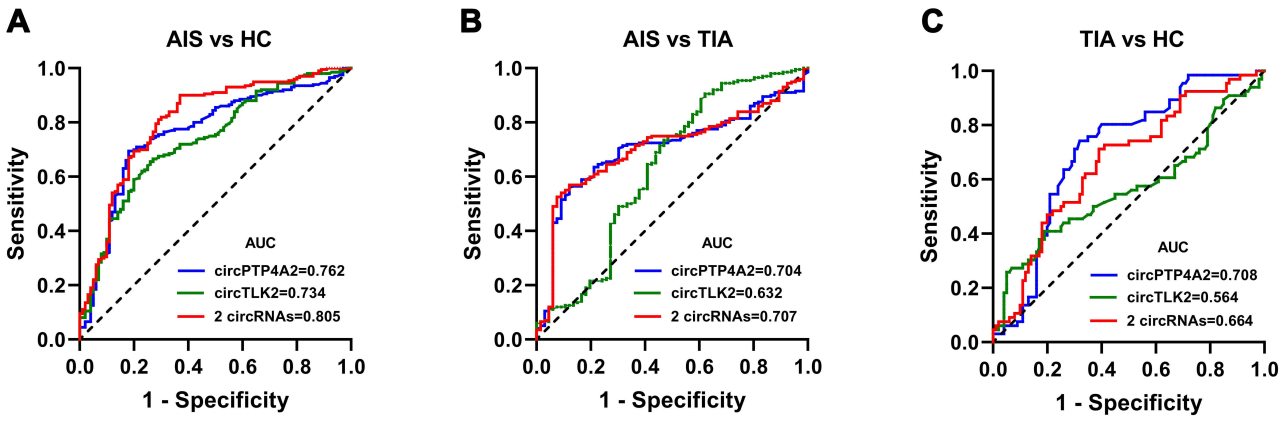

Figure 8 Diagnostic property of individual circRNAs and the combined circRNAs. Receiver operating characteristics (ROC) curves were calculated using the baseline levels of circRNAs based on the replication sample and their corresponding AUC values for discriminating AIS patients from HCs (**A**), for discriminating AIS patients from TIA patients (**B**), and for discriminating TIA patients from HCs (**C**).

Table 5 Diagnostic Property of Individual circRNAs and the Combined circRNAs

Variables	AUC (95% CI)	*P*-value	Sensitivity	Specificity
AIS patients vs HCs				
circPTP4A2	0.762 (0.703–0.820)	<0.001	0.695	0.820
circTLK2	0.734 (0.675–0.793)	<0.001	0.665	0.730
The combined circRNAs	0.805 (0.751–0.860)	<0.001	0.900	0.630
TIA patients vs HCs				
circPTP4A2	0.708 (0.628–0.787)	<0.001	0.742	0.680
circTLK2	0.564 (0.470–0.658)	0.164	0.409	0.810
The combined circRNAs	0.664 (0.580–0.748)	<0.001	0.580	0.748
AIS patients vs TIA patients				
circPTP4A2	0.704 (0.637–0.770)	<0.001	0.560	0.879
circTLK2	0.632 (0.546–0.719)	0.001	0.905	0.379
The combined circRNAs	0.707 (0.640–0.773)	<0.001	0.570	0.879

Abbreviations: AIS, acute ischemic stroke; AUC, area under the curve; CI, confidence interval; HCs, healthy control subjects; TIA, transient ischemic attack.

showed no significant difference compared with that in HCs. Additionally, the expression level of circTLK2 in AIS samples at Day 90 remained higher than that in HCs (P=0.041).

Discussion

Our study successfully constructed an AISIRC network and its associated subnetwork by using expression profiles and interaction information from the bioinformatics database. More importantly, we successfully identified and validated the distinctive expression signatures of two circRNAs (circPTP4A2 and circTLK2) that are differentially expressed after AIS. Multiple statistical evaluations indicated that these two circRNAs may be suitable for predicting and diagnosing the presence of AIS. In addition, both circPTP4A2 and circTLK2 showed good diagnostic value as assessed by ROC analysis, and reflected dynamic changes in AIS. We thus consider circPTP4A2 and circTLK2 to function as potential biomarkers for AIS diagnosis.

CircRNAs can serve as diagnostic biomarkers for AIS. Our previous study illustrated that circFUNDC1, circPDS5B, and circCDC14A expression levels increased in the plasma of AIS patients and could serve as biomarkers for the diagnosis and prognosis of AIS.[16] Dong et al[32] also demonstrated that 13 circRNAs are differentially expressed in the

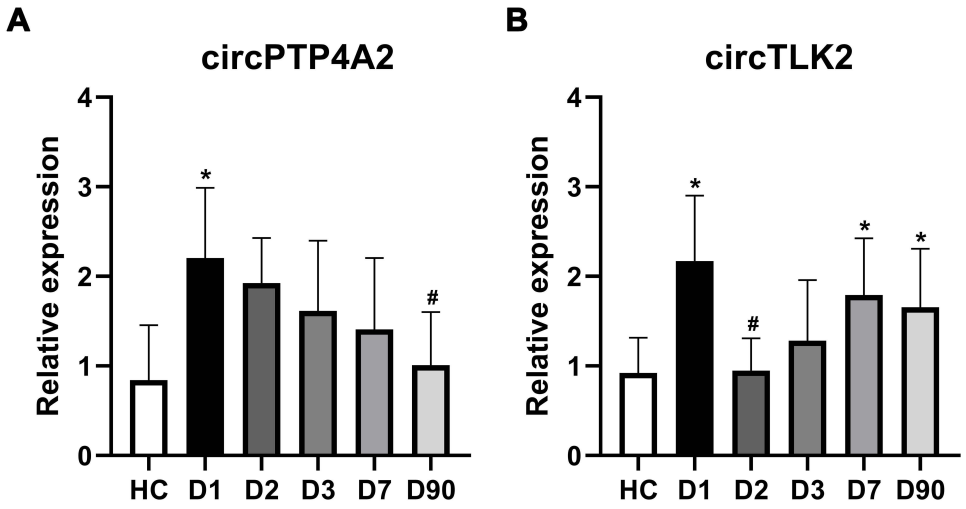

Figure 9 Temporal expression profile of validated circRNAs after AIS. The results for 18 patients with available data for five time points after AIS: circPTP4A2 (**A**) and circTLK2 (**B**). Median ± interquartile range, Kruskal–Wallis ANOVA test followed by Bonferroni correction pairwise comparisons. *P<0.05 compared with HC; #P<0.05 compared with day 1.

peripheral blood mononuclear cells (PBMCs) of patients with AIS by high-throughput sequencing and qRT-PCR. Nevertheless, the role of many circRNAs in AIS remains largely unstudied. In contrast to the aforementioned studies, we constructed a circRNA-mediated ceRNA network to explore immune-related circRNAs in AIS and confirmed their independent predictive ability for AIS.

Neuroinflammation and immune responses start a few minutes after AIS onset, become the major pathogenetic mechanisms within hours, and can last for several months to several years.[5,33] Recently, several studies found that circRNAs were involved in the pathogenesis of AIS by regulating immunoinflammatory reactions.[17,34,35] The circRNA-mediated ceRNA mechanism can be used for the analysis of the molecular basis of various diseases. Hence, constructing a ceRNA network of immune-related circRNAs should help elucidate the inflammatory mechanisms in AIS. In this study, we identified 548 DECs, 63 DEMs and 52 DEIRGs from databases, and analysed the functions of the DEIRGs. The GO enrichment analysis revealed that DEIRGs were mainly involved in immune-related BPs such as immune response-activating cell surface receptor signaling pathway, immune response-activating signal transduction, and neutrophil activation involved in immune response. Similarly, the KEGG pathway analysis of DEIRGs revealed several enriched immune-related pathways including cytokine–cytokine receptor interaction, primary immunodeficiency and Th17 cell differentiation. Then, we established the AISIRC network, including 15 DECs, 12 DEMs, 26 DEIRGs using DEM–DEIRG and DEM–DEC interaction pairs. Thus, these circRNAs from the AISIRC network may have important roles in the immune mechanisms of AIS. In addition, we constructed circRNA–miRNA–hub gene subnetworks and identified nine circRNAs that were closely related to immunoinflammation following AIS.

Next, we systematically validated the upregulated circRNAs from the circRNA–miRNA–hub gene subnetwork and identified two circRNAs (circPTP4A2 and circTLK2) that were confirmed in two independent sets. In addition, we determined the diagnostic values of circPTP4A2 and circTLK2 using logistic regression analysis combined with ROC curve analysis in AIS. To the best of our knowledge, the expression levels of these two circRNAs in plasma of AIS patients remain unclear. As such, the present study demonstrated for the first time that the levels of two immune-related circRNAs, namely circPTP4A2 and circTLK2, increased in AIS patients, and further focused on their potential clinical significance as diagnostic markers for AIS.

TIA is a major sign of impending stroke. The risk of stroke in TIA patients is as high as 10.5% within 90 days after the event.[36] Thus, an accurate and rapid diagnostic approach for TIA is crucial to reducing the risk of stroke. Importantly, our results revealed that the expression levels of circPTP4A2 were elevated in patients with TIA compared with HCs, and it might be an independent risk factor for predicting TIA. Although the logistic regression analysis indicated that increased circTLK2 was also closely associated with the presence of TIA, there was no significant difference between TIA patients and HCs in the replication sample. Moreover, the ROC curve analysis showed poor significance with an AUC value of 0.564 in distinguishing TIA patients from HCs according to the levels of circTLK2. Indeed, in actual clinical practice, a significant proportion of "stroke mimics" receive thrombolysis and admission to a stroke unit with high health care costs.[37] Thus, good diagnostic blood biomarkers of stroke should differentiate AIS patients not only from HCs but also from patients with stroke mimics, such as TIA. In this study, we observed that the levels of circPTP4A2 and circTLK2 in AIS patients were elevated compared with those in TIA patients. Moreover, the joint ROC curve for circPTP4A2 and circTLK2 demonstrated moderate accuracy in distinguishing TIA patients from AIS patients. Together, these results provide novel insights into the prediction and differentiation of TIA.

Currently, noncontrast head CT scans are typically the preferred imaging modality for AIS. Although previous studies have already described various early CT signs of AIS, these signs have poor sensitivity at the acute stage of stroke.[3] In this study, the combination of circPTP4A2 and circTLK2 showed higher sensitivity than CT. In addition, our results showed that the levels of these two circRNAs were elevated at early stages of AIS, and their peak expression appeared at admission (Day 1). In other words, peak expression of both circPTP4A2 and circTLK2 might be used to estimate the time of stroke onset and influence treatment decisions of patients with unknown time of onset, especially patients with wake-up stroke. Strikingly, the peaking of circPTP4A2 was followed by a gradual decay to control levels, whereas the expression level of circTLK2 in AIS samples at Day 90 remained higher. Therefore, we speculate that circTLK2 may still exert a biological action at the chronic stage after stroke. However, this requires further investigation to prove.

Understanding the molecular functions, interaction patterns and representative signalling pathways of identified circRNAs in AIS contributes to our knowledge of AIS pathogenesis. In the present study, based on the circRNA–miRNA–hub gene subnetworks, circPTP4A2, namely, hsa_circ_0007364, was involved in two ceRNA pathways, hsa_circ_0007364-hsa-miR-942-5p-FCGR3A and hsa_circ_0007364-hsa-miR-942-5p-FCGR3B. Furthermore, circTLK2, namely, hsa_circ_0045128, also acts as a ceRNA by sponging hsa-miR-942-5p to regulate FCGR3A and FCGR3B. According to previous studies, miR-942-5p could attenuate oxidative stress and inflammation in an in vivo atherosclerosis model.[38] IgG Fcγ receptors are encoded by FCGR3A and FCGR3B, which in turn mediate immune cell activation promoting inflammation.[39] Regrettably, there is no evidence in the literature that the RNA molecules described above may be involved in the neuroinflammation of AIS. In summary, circPTP4A2-mediated and circTLK2-mediated ceRNA networks represent valuable research tools to further investigate the inflammatory mechanisms of circPTP4A2/ circTLK2 in AIS, and follow-up research will be implemented in the future.

However, the present study has limitations that merit comment. First, the expression data are not from the same dataset. In other words, we could not overcome the heterogeneity challenges of comprehensive analysis from different platforms. Moreover, due to inconsistent annotations across databases, some data might be missing during the process of data integration. Second, all of the participants came from the same hospital in China, which limits the generalization of the results. Thus, further randomized multicenter studies are required to validate these findings. Third, this study only focused on the diagnostic value of circRNAs and lacked follow-up data on the prognostic value of circRNAs in AIS patients, which hampered the broader understanding of AIS prevention and treatment. Fourth, the underlying mechanisms of circPTP4A2 and circTLK2 were solely predicted by bioinformatics analysis and further functional experiments should be conducted to validate the circRNA-mediated ceRNA axis for immunomodulation of AIS.

Conclusion

In conclusion, we established an immune-related circRNA–miRNA–gene network, which provided a novel strategy for elucidating the molecular basis and exploring emerging diagnostic tools for AIS. These circRNAs acting as ceRNAs may serve as new diagnostic targets for AIS. Furthermore, we illustrated circPTP4A2 and circTLK2 expression signatures in AIS and TIA patients. These two circulating circRNAs manifested diagnostic potentials with higher sensitivity than CT, and thus they could serve as promising biomarkers for AIS.

Data Sharing Statement

All data supporting our results are available from the corresponding authors upon reasonable.

Ethics Approval and Informed Consent

This experimental protocol was reviewed and approved by the Ethics Committee of the Affiliated Hospital of Xuzhou Medical University (approval ID: XYFY2021-KL107-01) and conducted in compliance with the ethical principles expressed in the Declaration of Helsinki, and this study was registered at the US National Institutes of Health (NIH) Clinical Trials Registry (Identifier: NCT 05098340). Written informed consent was obtained from all subjects or their legally authorized representatives.

Author Contributions

All authors made a significant contribution to the work reported, whether that is in the conception, study design, execution, acquisition of data, analysis and interpretation, or in all these areas; took part in drafting, revising or critically reviewing the article; gave final approval of the version to be published; have agreed on the journal to which the article has been submitted; and agree to be accountable for all aspects of the work.

Funding

This work was supported by the National Natural Science Foundation of China (Grant No. 82071325) and the Science and Technology Planning Project of Xuzhou, China (Grant No. KC20113).

Disclosure

The authors report no conflicts of interest in this work.

References

1. Wu S, Wu B, Liu M, et al. Stroke in China: advances and challenges in epidemiology, prevention, and management. *Lancet Neurol*. 2019;18(4):394–405. doi:10.1016/S1474-4422(18)30500-3
2. Zhou M, Wang H, Zeng X, et al. Mortality, morbidity, and risk factors in China and its provinces, 1990–2017: a systematic analysis for the Global Burden of Disease Study 2017. *Lancet*. 2019;394(10204):1145–1158. doi:10.1016/S0140-6736(19)30427-1
3. Bonney PA, Walcott BP, Singh P, Nguyen PL, Sanossian N, Mack WJ. The continued role and value of imaging for acute ischemic stroke. *Neurosurgery*. 2019;85(suppl_1):S23–S30. doi:10.1093/neuros/nyz068
4. Easton JD, Saver JL, Albers GW, et al. Definition and evaluation of transient ischemic attack: a scientific statement for healthcare professionals from the American Heart Association/American Stroke Association Stroke Council; Council on Cardiovascular Surgery and Anesthesia; Council on Cardiovascular Radiology and Intervention; Council on Cardiovascular Nursing; and the Interdisciplinary Council on Peripheral Vascular Disease. The American Academy of Neurology affirms the value of this statement as an educational tool for neurologists. *Stroke*. 2009;40(6):2276–2293. doi:10.1161/STROKEAHA.108.192218
5. Iadecola C, Buckwalter MS, Anrather J. Immune responses to stroke: mechanisms, modulation, and therapeutic potential. *J Clin Invest*. 2020;130(6):2777–2788. doi:10.1172/JCI135530
6. Maida CD, Norrito RL, Daidone M, Tuttolomondo A, Pinto A. Neuroinflammatory mechanisms in ischemic stroke: focus on cardioembolic stroke, background, and therapeutic approaches. *Int J Mol Sci*. 2020;21(18):6454. doi:10.3390/ijms21186454
7. Mengozzi M, Kirkham FA, Girdwood EER, et al. C-reactive protein predicts further ischemic events in patients with transient ischemic attack or lacunar stroke. *Front Immunol*. 2020;11:1403. doi:10.3389/fimmu.2020.01403
8. Jenny NS, Callas PW, Judd SE, et al. Inflammatory cytokines and ischemic stroke risk: the REGARDS cohort. *Neurology*. 2019;92(20):e2375–e2384. doi:10.1212/WNL.0000000000007416
9. Katan M, Moon YP, Paik MC, et al. Procalcitonin and midregional proatrial natriuretic peptide as markers of ischemic stroke: the Northern Manhattan study. *Stroke*. 2016;47(7):1714–1719. doi:10.1161/STROKEAHA.115.011392
10. Palm F, Pussinen PJ, Safer A, et al. Serum matrix metalloproteinase-8, tissue inhibitor of metalloproteinase and myeloperoxidase in ischemic stroke. *Atherosclerosis*. 2018;271:9–14. doi:10.1016/j.atherosclerosis.2018.02.012
11. Xin R, Gao Y, Gao Y, et al. isoCirc catalogs full-length circular RNA isoforms in human transcriptomes. *Nat Commun*. 2021;12(1):266. doi:10.1038/s41467-020-20459-8
12. Mehta SL, Dempsey RJ, Vemuganti R. Role of circular RNAs in brain development and CNS diseases. *Prog Neurobiol*. 2020;186:101746. doi:10.1016/j.pneurobio.2020.101746
13. Hansen TB, Jensen TI, Clausen BH, et al. Natural RNA circles function as efficient microRNA sponges. *Nature*. 2013;495(7441):384–388. doi:10.1038/nature11993
14. Yang J, Cheng M, Gu B, Wang J, Yan S, Xu D. CircRNA_09505 aggravates inflammation and joint damage in collagen-induced arthritis mice via miR-6089/AKT1/NF-κB axis. *Cell Death Dis*. 2020;11(10):833. doi:10.1038/s41419-020-03038-z
15. Chen J, Yang X, Liu R, et al. Circular RNA GLIS2 promotes colorectal cancer cell motility via activation of the NF-kappaB pathway. *Cell Death Dis*. 2020;11(9):788. doi:10.1038/s41419-020-02989-7
16. Zuo L, Zhang L, Zu J, et al. Circulating circular RNAs as biomarkers for the diagnosis and prediction of outcomes in acute ischemic stroke. *Stroke*. 2020;51(1):319–323. doi:10.1161/STROKEAHA.119.027348
17. Zuo L, Xie J, Liu Y, Leng S, Zhang Z, Yan F. Down-regulation of circular RNA CDC14A peripherally ameliorates brain injury in acute phase of ischemic stroke. *J Neuroinflammation*. 2021;18(1):283. doi:10.1186/s12974-021-02333-6
18. Barr TL, Conley Y, Ding J, et al. Genomic biomarkers and cellular pathways of ischemic stroke by RNA gene expression profiling. *Neurology*. 2010;75(11):1009–1014. doi:10.1212/WNL.0b013e3181f2b37f
19. Tiedt S, Prestel M, Malik R, et al. RNA-Seq identifies circulating miR-125a-5p, miR-125b-5p, and miR-143-3p as potential biomarkers for acute ischemic stroke. *Circ Res*. 2017;121(8):970–980. doi:10.1161/CIRCRESAHA.117.311572
20. Bhattacharya S, Dunn P, Thomas CG, et al. ImmPort, toward repurposing of open access immunological assay data for translational and clinical research. *Sci Data*. 2018;5:180015. doi:10.1038/sdata.2018.15
21. Breuer K, Foroushani AK, Laird MR, et al. InnateDB: systems biology of innate immunity and beyond–recent updates and continuing curation. *Nucleic Acids Res*. 2013;41(Databaseissue):D1228–1233. doi:10.1093/nar/gks1147
22. Glažar P, Papavasileiou P, Rajewsky N. circBase: a database for circular RNAs. *RNA*. 2014;20(11):1666–1670. doi:10.1261/rna.043687.113
23. Kozomara A, Birgaoanu M, Griffiths-Jones S. miRBase: from microRNA sequences to function. *Nucleic Acids Res*. 2019;47(D1):D155–D162. doi:10.1093/nar/gky1141
24. Ritchie ME, Phipson B, Wu D, et al. limma powers differential expression analyses for RNA-sequencing and microarray studies. *Nucleic Acids Res*. 2015;43(7):e47. doi:10.1093/nar/gkv007
25. Wu T, Hu E, Xu S, et al. clusterProfiler 4.0: a universal enrichment tool for interpreting omics data. *Innovation*. 2021;2(3):100141. doi:10.1016/j.xinn.2021.100141
26. Sticht C, De La Torre C, Parveen A, Gretz N. miRWalk: an online resource for prediction of microRNA binding sites. *PLoS One*. 2018;13(10):e0206239. doi:10.1371/journal.pone.0206239
27. Liu M, Wang Q, Shen J, Yang BB, Ding X. Circbank: a comprehensive database for circRNA with standard nomenclature. *RNA Biol*. 2019;16(7):899–905. doi:10.1080/15476286.2019.1600395
28. Tay Y, Rinn J, Pandolfi PP. The multilayered complexity of ceRNA crosstalk and competition. *Nature*. 2014;505(7483):344–352. doi:10.1038/nature12986
29. Shannon P, Markiel A, Ozier O, et al. Cytoscape: a software environment for integrated models of biomolecular interaction networks. *Genome Res*. 2003;13(11):2498–2504. doi:10.1101/gr.1239303

30. Szklarczyk D, Gable AL, Nastou KC, et al. The STRING database in 2021: customizable protein-protein networks, and functional characterization of user-uploaded gene/measurement sets. *Nucleic Acids Res*. 2021;49(D1):D605–D612. doi:10.1093/nar/gkaa1074
31. Scardoni G, Petterlini M, Laudanna C. Analyzing biological network parameters with CentiScaPe. *Bioinformatics*. 2009;25(21):2857–2859. doi:10.1093/bioinformatics/btp517
32. Dong Z, Deng L, Peng Q, Pan J, Wang Y. CircRNA expression profiles and function prediction in peripheral blood mononuclear cells of patients with acute ischemic stroke. *J Cell Physiol*. 2020;235(3):2609–2618. doi:10.1002/jcp.29165
33. Zhang SR, Phan TG, Sobey CG. Targeting the immune system for ischemic stroke. *Trends Pharmacol Sci*. 2021;42(2):96–105. doi:10.1016/j.tips.2020.11.010
34. Han B, Zhang Y, Zhang Y, et al. Novel insight into circular RNA HECTD1 in astrocyte activation via autophagy by targeting MIR142-TIPARP: implications for cerebral ischemic stroke. *Autophagy*. 2018;14(7):1164–1184. doi:10.1080/15548627.2018.1458173
35. Yang L, Han B, Zhang Z, et al. Extracellular vesicle-mediated delivery of circular RNA SCMH1 promotes functional recovery in rodent and nonhuman primate ischemic stroke models. *Circulation*. 2020;142(6):556–574. doi:10.1161/CIRCULATIONAHA.120.045765
36. Johnston SC, Gress DR, Browner WS, Sidney S. Short-term prognosis after emergency department diagnosis of TIA. *JAMA*. 2000;284(22):2901–2906. doi:10.1001/jama.284.22.2901
37. Ali-Ahmed F, Federspiel JJ, Liang L, et al. Intravenous tissue plasminogen activator in stroke mimics. *Circ Cardiovasc Qual Outcomes*. 2019;12(8):e005609. doi:10.1161/CIRCOUTCOMES.119.005609
38. Wan H, You T, Luo W. circ_0003204 regulates cell growth, oxidative stress, and inflammation in ox-LDL-induced vascular endothelial cells via regulating miR-942-5p/HDAC9 axis. *Front Cardiovasc Med*. 2021;8:646832. doi:10.3389/fcvm.2021.646832
39. Ravetch JV, Bolland S. IgG Fc receptors. *Annu Rev Immunol*. 2001;19:275–290. doi:10.1146/annurev.immunol.19.1.275